Developmental Biology 456 (2019) 201–211

Contents lists available at ScienceDirect

Developmental Biology

journal homepage: www.elsevier.com/locate/developmentalbiology

Original research article

Cytoskeletal polarization and cytokinetic signaling drives polar lobe formation in spiralian embryos

Leslie Toledo-Jacobo [a,b], John H. Henson [b,c], Charles B. Shuster [a,b,*]

[a] Department of Biology, New Mexico State University, Las Cruces, NM, 88003, USA
[b] University of Washington Friday Harbor Laboratories, Friday Harbor, WA, 98250, USA
[c] Department of Biology, Dickinson College, Carlisle, PA, 17013, USA

ARTICLE INFO

Keywords:
Polar lobe
Cytokinesis
Arp2/3
Mollusk
Spiralian
Embryo

ABSTRACT

In many spiralians, asymmetry in the first two cleavages is achieved through the formation of a polar lobe (PL), which transiently constricts to sequester vegetal cytoplasm into the CD and D blastomeres. While microtubules and actin filaments are required for polar lobe formation, little else is known regarding the structural and functional similarities with the contractile ring, or how the PL constriction is able to form perpendicular to the cleavage plane. Examination of scallop embryos revealed that while activated myosin II could be detected in both the cleavage furrow and early PL constriction, astral or central spindle microtubules were not observed associated with the PL neck until the constriction was nearly complete. Further, inhibition of Aurora B had no effect on polar lobe initiation, but blocked both contractile ring ingression and PL constriction beyond phase II. The cortex destined for PL sequestration was marked by enrichment of the Arp2/3 complex, which was first detected during meiosis and remained enriched at the vegetal pole through the first two cleavages. Inhibition of Arp2/3 affected PL formation and partitioning of cytoplasm into the two daughter cells, suggesting that Arp2/3 plays a functional role in defining the zone of cortex to be sequestered into the polar lobe. Together, these data offer for the first time a mechanism by which a cytoskeletal specialization defines the polar lobe in this atypical form of asymmetric cell division.

1. Introduction

Asymmetric cell division is a hallmark of many embryonic and stem cell divisions (Morin and Bellaïche, 2011). During early embryogenesis, asymmetric cell fates depend on the differential segregation of developmental determinants amongst the daughter blastomeres. Embryos may cleave asymmetrically by positioning the mitotic spindle towards one pole of the cell, or by forming asters of unequal sizes (Lu and Johnston, 2013). However, some species of mollusks and annelids achieve asymmetric cell division through the formation of a transient vegetal protrusion called the polar lobe (PL). Also known as antipolar or yolk lobes, PLs form during the first and second embryonic divisions, sequestering vegetal cytoplasm that is inherited by the CD and D blastomeres, respectively (Clement, 1952; Crampton and Wilson, 1896; Morgan, 1933). While the developmental roles of the PL have been studied in a number of spiralian embryos, little is known about how the polar lobe constriction is related to the contractile ring or how the PL is regulated in space and time.

Experimental manipulation of PLs date back to the 19th century (Crampton and Wilson, 1896), and since then many investigators have studied the developmental consequences of lobe removal through microsurgery. Removing the PL in *Ilyanassa obsoleta* embryos leads to a symmetric first cell division and the resulting larva fails to form a heart, intestine, foot, operculum, statocysts, eyes, and shell (Atkinson, 1971; Clement, 1952; Crampton and Wilson, 1896; Render, 1989) and similar results were observed in *Bithynia tentaculata* (Cather and Verdonk, 1974). Removal of the PL in *Dentalium* results in a larva lacking the apical tuft and the post-trochal region (Wilson, 1904), whereas experimental equalization of the first cleavage in *Dentalium* (Guerrier et al., 1978), *Sabellaria* (Novikoff, 1940) and *Chaetopterus* (Tyler, 1930) gives rise to a larva with duplications in dorsal structures. In contrast to *Ilyanassa, Sabellaria, and Dentalium*, the polar lobes of *Crepidula fornicata,* sequesters less than 1% of cell volume, and PL removal has no effect on dorsoventral axis specification (Henry et al., 2006). Similarly, removal of the small PL in *Chaetopterus variopedatus* leads to a morphologically normal larva, except that its photocytes are unable to emit light (Henry, 1989). It has

* Corresponding author. Department of Biology, New Mexico State University, Las Cruces, NM, 88003-8001, USA.
E-mail addresses: leslietj@nmsu.edu (L. Toledo-Jacobo), henson@dickinson.edu (J.H. Henson), cshuster@nmsu.edu (C.B. Shuster).

https://doi.org/10.1016/j.ydbio.2019.08.020
Received 28 May 2019; Received in revised form 15 July 2019; Accepted 28 August 2019
Available online 31 August 2019

been hypothesized that the PL of *Crepidula* may contribute to the regulation and activation of MAPK for the specification of the 3D macromere (Henry et al., 2017), but little else is known regarding the exact developmental determinants sequestered by this structure. And just as the developmental role of the polar lobe remains poorly understood, little is known about the mechanics of polar lobe formation.

The polar lobe forms through a Polar Lobe Constriction (PLC) of the vegetal cortex that ingresses perpendicular to the plane of cleavage, and filamentous actin has been shown to be enriched in both the PLC and contractile ring (Conrad and Williams, 1974; Conrad et al., 1973; Hejnol and Pfannenstiel, 1998; Schmidt et al., 1980). Disruption of actin filaments with cytochalasin B or Latrunculin B prevents the formation of both the contractile ring and PLC, or causes their regression if they have already formed (Conrad and Williams, 1974; Raff, 1972). Another parallel between the contractile ring and the PLC is the requirement for myosin II activity (Hejnol and Pfannenstiel, 1998). The role of microtubules is less clear. Astral microtubules of the mitotic apparatus specify the equatorial position of the contractile ring (Rappaport, 1996) through the action of protein complexes that direct the Rho-dependent contractile ring assembly (Glotzer, 2005, 2009), but the PL constricts in a plane perpendicular to the cell equator. While MT depolymerization prior to cleavage furrow or PLC initiation inhibits polar lobe ingression, early initiation of the PLC (referred to as Phase I) is unaffected, and later treatments affect the reabsorption of the PL only (Conrad and Conrad, 1992; Conrad and Williams, 1974). Conversely, microtubule stabilization maintains the PLC and prevents polar lobe reabsorption (Conrad et al., 1992, 1994). Thus, while the polar lobe constriction resembles the contractile ring in many respects, the geometry of the PLC with respect to the cleavage plane as well as its partial dependence on microtubules raises questions as to the spatial and temporal regulation of this actomyosin structure.

The formation and importance of the polar lobe has been a subject of

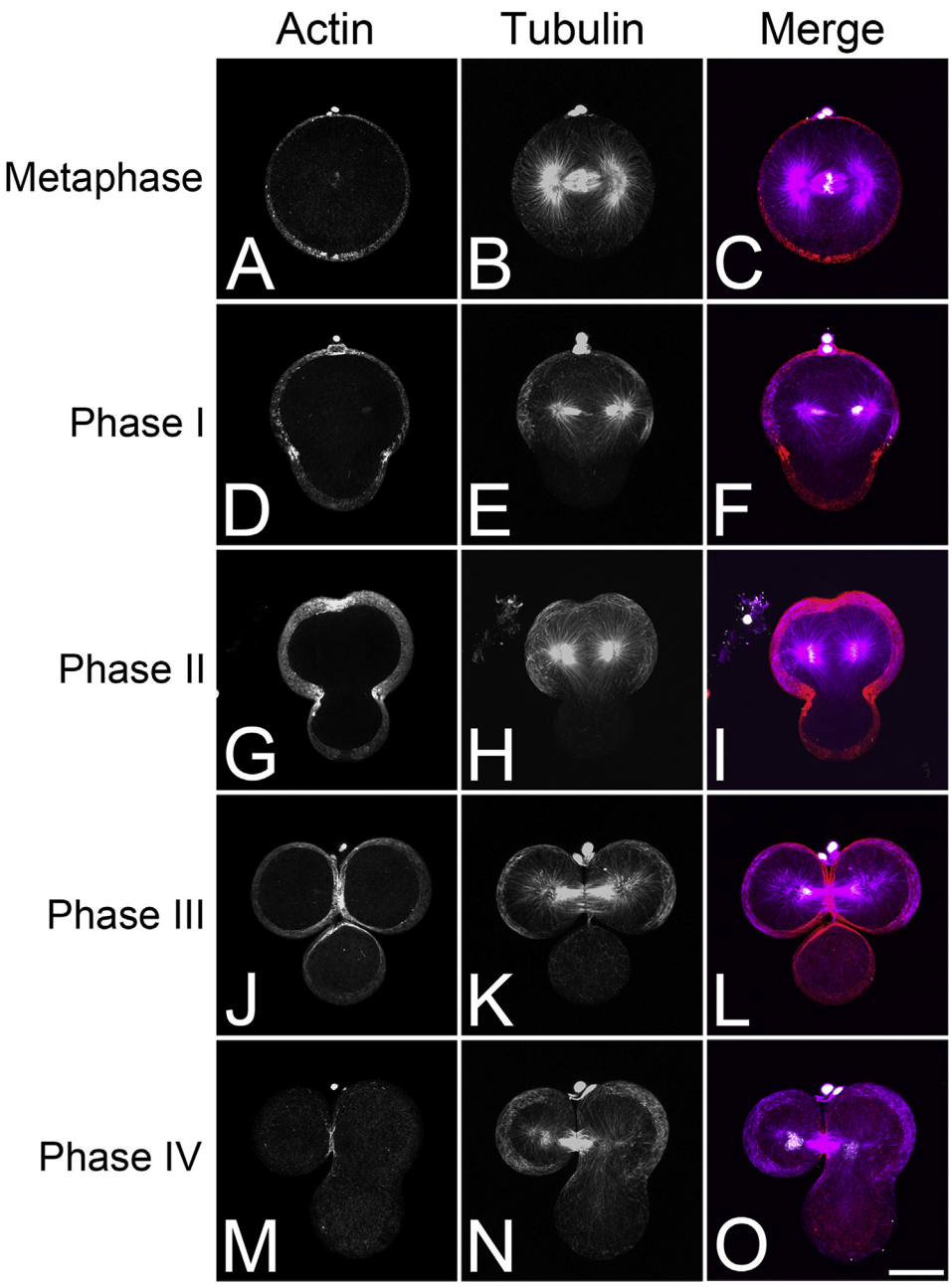

Fig. 1. Actin and microtubule distribution during polar lobe formation and first division in the scallop *C. hastata*. Projection images of *C. hastata* embryos probed for microtubules (magenta), F-actin (red) and DNA (white). Bar, 30 μm.

interest and speculation for over a century, and while the developmental role of polar lobes have been identified in some species, the mechanisms by which this constriction forms in apparent violation of the normal rules of cleavage plane determination are unknown. We studied polar lobe formation in scallop embryos and found that the partial dependence of MT's on PLC formation was associated with the activity of the Chromosomal Passenger Complex (CPC), which plays a key role in regulating post-anaphase MT organization and cytokinetic signaling (Carmena et al., 2012). Moreover, we found that the vegetal cortex destined to be sequestered within the polar lobe was defined by the Arp 2/3 complex, which nucleates the polymerization of branched actin networks (Rotty et al., 2013) and that inhibition of Arp2/3 disrupted polar lobe formation and asymmetric cell division. In summary, these studies provide the first mechanistic insights underlying this highly atypical form of asymmetric cell division during early development and raise new questions regarding how Arp2/3 polarization is initiated during meiosis as well as how it is downregulated following the second cleavage.

2. Results

2.1. Organization of the actomyosin and microtubule cytoskeletons during polar lobe formation in the scallop embryo

Polar lobe formation in *Ilynassa* is described as occurring in four phases (Conrad and Williams, 1974) and in an effort to better understand this process in a more optically clear embryo, we examined polar lobe formation in two closely related species of scallops (*Chlamys hastada* and *C. rubida*). Examination of fixed *Chlamys* embryos revealed that polar lobe progression closely paralleled what has been described for *Illynassa*. Phase I initiated with a vegetal elongation of the zygote, followed by a slow reduction in the diameter of the PL neck (Fig. 1D–F). Phase II constriction coincided with initiation of the cleavage furrow with the diameter of the PL neck rapidly constricting in a linear manner (Fig. 1G–I). Maximum constriction of the PLC occurred in Phase III (or trefoil stage), when the cleavage furrow had nearly ingressed to completion (Fig. 1J-L). Finally, during Phase IV, the PLC relaxed (Fig. 1M–O), releasing the contents of the polar lobe into the CD blastomere.

Visualization of F-actin revealed that actin enrichment within the plane of the forming PL could be observed as early as phase I (Fig. 1D–F), and during phases II and III, actin enrichment increased in both the contractile ring and PL as both constrictions ingressed (Fig. 1G-L). During Phase IV, F-actin at the PLC was dramatically reduced whereas F-actin within the contractile ring remained (Fig. 1M–O). Immunolabeling for active myosin II (phospho-Ser19-myosin regulatory light chain, PMLC) revealed that prior to phase I, phosphomyosin was largely confined to the site of polar body extrusion (Fig. 2A, arrowhead) but in early Phase I, a belt of phosphomyosin could be observed at the future sites of both the contractile ring and PLC (Fig. 2B). During phases I and II, phosphomyosin accumulated as broad, intersecting perpendicular bands at the planes of the contractile ring and PLC (Fig. 2B and C). During phase III, both zones of active myosin narrowed considerably (Fig. 2D and E), with the PLC ingressing nearly to completion in trefoil embryos (Fig. 2E, arrowhead). And as was observed for F-actin (Fig. 1M), by phase IV, phosphomyosin was absent from the regressing PLC, being only maintained in the contractile ring (Fig. 2F).

The PLC formed perpendicular to the contractile ring during the first cleavage of *Chlamys* embryos (Figs. 1 and 2), in apparent violation of the geometric relationship between the mitotic spindle and cleavage plane in animal cells, which predicts that the contractile ring assembles at the midpoint between the two spindle poles (Rappaport, 1996). Post-anaphase microtubules of the mitotic spindle determine the cleavage plane in animal cells by recruiting the signaling machinery that activates Rho and assembly of the contractile ring (Bement et al., 2005; D'Avino et al., 2005), and in early embryos, it is overlapping astral microtubules that recruit these factors (Argiros et al., 2012). To better understand the spatial relationship between microtubules and the PLC, embryos were probed for microtubule morphology and imaged using Super Resolution Radial Fluctuation (SRRF) microscopy (Fig. 3), which affords sub-diffraction limit imaging (Culley et al., 2018; Gustafsson et al., 2016). In early anaphase, astral microtubules extended toward the vegetal pole, but did not extend deep into the cytoplasm where the PLC will form (Fig. 3A). These vegetal astral microtubules were maintained during phase II (Fig. 3B) and became physically associated with the PLC during phase III, but never extended past the constriction (Fig. 3C). These microtubules appeared to condense and bundle, resembling the microtubule arrays of the adjacent central spindle (Fig. 3C). As the PLC relaxed, these astral microtubules extended further into the polar lobe (Fig. 3D and E).

Experiments with microtubule-destabilizing drugs suggest that

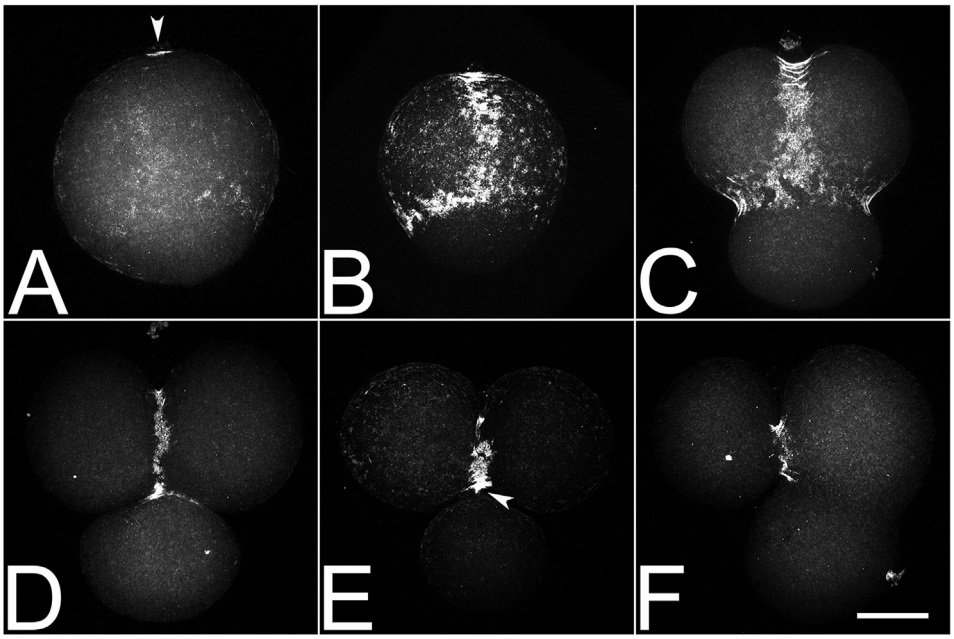

Fig. 2. Active myosin II is localized at the cleavage furrow and polar lobe constriction in *C. hastata* early embryos. Projection images of *C. hastata* embryos fixed and probed for Ser19-Phosphorylated Myosin regulatory Light Chain (PMLC). PMLC was initially restricted to the site of polar body extrusion in the animal pole (A, arrowhead), but at the onset of phase I, PMLC accumulated at the future site of the contractile ring and PLC (B). PMLC was enriched at the cleavage furrow and PL constriction site during phase II and III (C–D). Late in phase III when the PLC had nearly ingressed to completion, PMLC is still present (E, arrowhead), but by phase IV, PMLC is lost from the polar lobe neck (F). Bar, 30 μm.

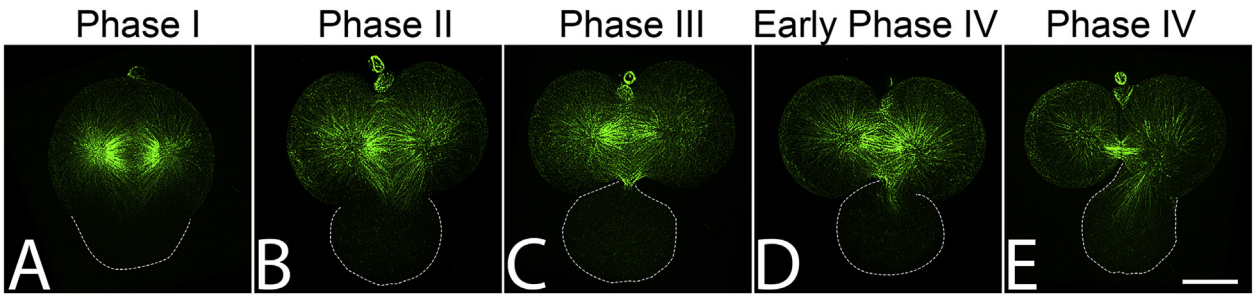

Fig. 3. Organization of microtubules associated with the PLC. *C. hastata* embryos were fixed and probed for microtubules and imaged by SRRF microscopy. Beginning at Phase II, a population of vegetally-oriented astral microtubules become bundled together by the trefoil stage (Phase III) (B–C). Once the PLC relaxes during phase IV, the astral microtubules of one spindle pole resume extending into polar lobe (D and E). Dashed lines indicate the boundary of the polar lobe. Bar, 30 μm.

during phase I, PLC formation is microtubule-independent, but by phase II, continued constriction of the PLC is microtubule-dependent (Conrad et al., 1992; Conrad and Conrad, 1992; Conrad and Williams, 1974). Given the close association of microtubules with the PLC and the close proximity of the PLC to the central spindle by phase III, we asked if PLC-associated microtubules had characteristics of central spindle microtubules that might suggest a functional role in promoting polar lobe constriction. Central spindle microtubules are more stable than astral microtubules in sea urchin embryos (Foe and von Dassow, 2008), and to test whether PLC-associated microtubules were similarly stable, embryos were briefly treated with high doses of nocodazole prior to processing for microtubule localization (Fig. 4). As expected, nocodazole treatment depolymerized cortical and astral microtubule, whereas the microtubules of the central spindle were preferentially stabilized (Fig. 4D–F). However, those microtubules associated with the PLC during phase III and IV (Fig. 4B and C) were not stable in the presence of nocodazole (Fig. 4E and F). Thus, the astral microtubules associated with the PLC were not likely stabilized by the components of the central spindle.

2.2. Role of cytokinetic signaling in polar lobe constriction

During animal cell cytokinesis, microtubules deliver factors to the cell equator that specify the position of the contractile ring, and these same factors organize central spindle microtubules into an antiparallel array (Glotzer, 2009; White and Glotzer, 2012). Prior work in *Ilyanassa* established that microtubules are required from Phase II onward (Conrad et al., 1992, 1994; Conrad and Conrad, 1992). The intersecting zones of active myosin (Fig. 2) and proximity of the central spindle to the PLC (Fig. 3) suggested that once the PLC began to ingress, the signaling apparatus associated with the central spindle might promote or maintain the PLC. To further explore this notion, embryos were cultured in the presence of DMSO or an inhibitor of Aurora B kinase, the catalytic constituent of the Chromosomal Passenger Complex (CPC), and an upstream regulator of central spindle assembly and cytokinesis (Guse et al., 2005). The small molecule inhibitor ZM447439 binds the conserved ATP-binding pocket of Aurora B, and blocks not only chromosome biorientation, chromosome segregation and cytokinesis (Ditchfield et al., 2003) but also the maintenance of chromatin condensation through histone phosphorylation (Gadea and Ruderman, 2005). Indeed, ZM447439 lowered phosphohistone H3 levels in scallop oocytes (Fig. S1), in a manner similar to what has been previously reported for Aurora inhibitors in echinoderm eggs (Argiros et al., 2012) and mollusk oocytes (George et al., 2006). When embryos were treated after the extrusion of the second polar body, DMSO-treated embryos underwent two successive rounds of polar lobe formation and cytokinesis normally (Fig. 5A–G, Supplemental Movie 1). However, in the absence of Aurora kinase activity, cytokinesis invariably failed in both first and second cleavages (Fig. 5H-N). Interestingly, the initiation of polar lobe constriction occurred normally, but did not advance past phase II (Fig. 5I–K, Supplemental Movie 2). PLCs halted in early phase II, and then

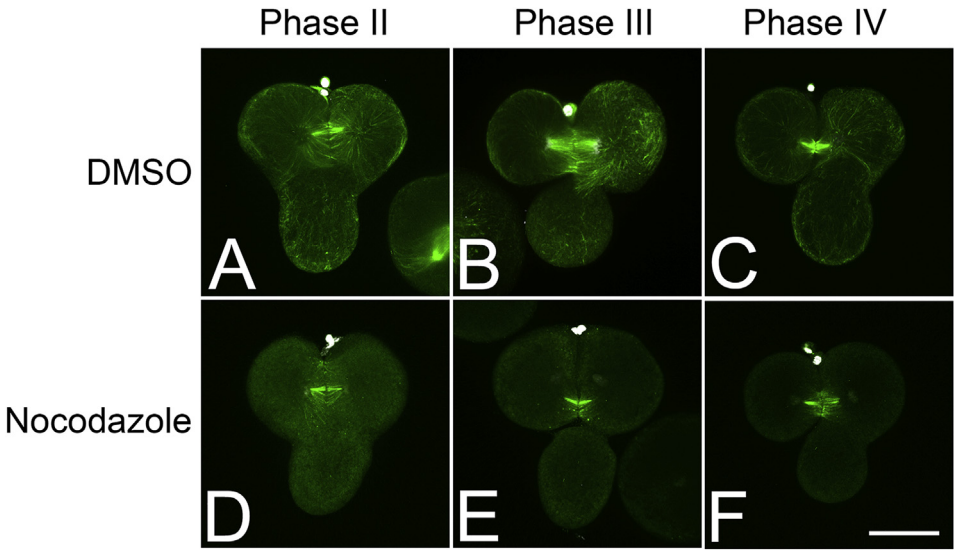

Fig. 4. Relative stability of microtubules of the central spindle and PLC. *C. rubida* embryos were briefly treated (2 min) with 0.1% DMSO (A–C) or 25 μM nocodazole (D–F) prior to fixation and processing for microtubule (green) and DNA (white) localization. Treatment with nocodazole revealed that lobe-associated microtubules were not resistant to depolymerization, and only the central spindle microtubules remained stable. Bar, 30 μm.

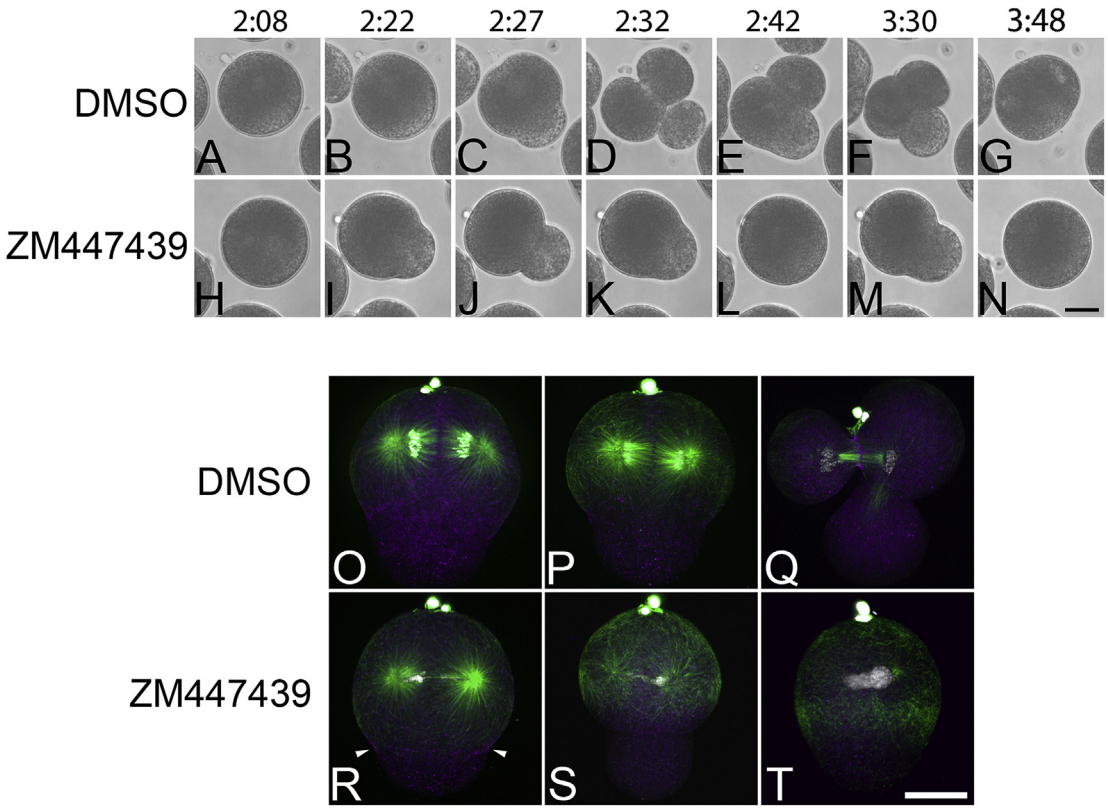

Fig. 5. Polar lobe constriction requires cytokinetic signaling. A-N) Following second meiosis, *C. rubida* embryos were treated with either 0.1% DMSO (A–G) or 50 μM ZM447439 (H–N) to block Aurora B signaling and cytokinesis. Embryos were then recorded in bright field microscopy. While treatment did not affect phase I polar lobe constriction, the PLC did not progress past phase II and retracted for both the first and second divisions. Polar lobe initiation was quantified for the first division with >50 cells per experiment (five experimental replicates), and no significant differences in polar lobe initiation were noted ($p = 0.4819$, two-tailed *t*-test). Time denotes hours and minutes post-fertilization. Bar, 30 μm. **O-T)** Morphology of DMSO and ZM447439-treated embryos treated as described in A-N and probed for microtubules (green), PMLC (magenta, arrows), DNA (white). While aurora inhibition resulted in chromosome segregation defects and cytokinesis failure, initiation of polar lobe formation was unaffected (R–T) suggesting that initiation of the lobe constriction was independent of canonical cytokinesis signaling pathways. Bar, 30 μm.

relaxed, only to reinitiate at the normal time during the second cleavage (Fig. 5K-M). Quantification of polar lobe initiation over five experimental replicates revealed no statistically significant differences between ZM447439-treated and control embryos ($p = 0.4819$), and polar lobe constrictions in treated embryos regressed with normal timing at the end of cell division (Fig. 5K-N). Finally, examination of cell morphology revealed that in contrast to controls (Fig. 5O–Q), Aurora B-inhibited cells exhibited chromosomal segregation and cytokinesis defects (Fig. 5R–T) consistent with known functions attributed to Aurora B (Carmena, 2008). Treated embryos were still able to assemble a bipolar spindle but were unable to form a central spindle (Fig. 5R,S). However, these embryos were still able to initiate Phase I polar lobe constrictions (Fig. 5R,S), further supporting the notion that the early initiation and ingression of the PLC was independent of spatial information imparted by the mitotic spindle. However, the more rapid and robust ingression observed during phases II and III appeared to be dependent on signals originating from the central spindle.

Supplementary video related to this article can be found at https://doi.org/10.1016/j.ydbio.2019.08.020.

2.3. Arp 2/3 delimits the zone of vegetal cortex destined to form the polar lobe, and is required for proper asymmetric cell division

Even though proper microtubule dynamics are necessary for PL constriction and relaxation, neither microtubules (Conrad et al., 1994; Conrad and Conrad, 1992; Raff, 1972) nor cytokinetic signaling machinery (Fig. 5) are required for PL initiation, positioning or timing. Moreover, the PL always forms at the vegetal pole independently of changes in the position of the contractile ring (Conrad et al., 1973), suggesting that there was another mechanism specifying the position of the polar lobe. When screening for cytoskeletal markers of the polar lobe constriction, we found that Arp2/3 was specifically localized at the vegetal cortex and polar lobe of *Chlamys* embryos (Figs. 6–7. S2–S3). In germinal vesicle stage *Chlamys* oocytes, Arp2/3 was found throughout the cortex (Figs. S2A–B). However, once oocytes entered meiosis I, Arp2/3 could be observed in the vegetal cortex of the oocyte through meiosis II (Figs. S2C–H). During the first cleavage of *Chlamys* embryos, Arp2/3 was increasingly enriched in the PL cortex, but also accumulated at the polar regions during cytokinesis (Fig. 6E–H). During phase IV, when the PLC relaxes and actin and active myosin II were lost from the polar lobe neck (Figs. 1 and 2), vegetal Arp2/3 localization was maintained (Fig. 6I and J). This localization pattern was maintained between the first and second divisions (Fig. 6K,L) and through the second cleavage (Fig. 6K-N) only to dissipate at the four-cell stage (Fig. 6O,P). A nearly identical localization pattern could be observed in the oyster *Crassostrea gigas* (Fig. S3), suggesting that this was not specifically a phenomenon restricted to scallop embryos.

In cells crawling in two dimensional environments, Arp2/3 and myosin II are typically found in spatially and biophysically distinct domains (Blanchoin et al., 2014). Indeed, co-localization of Arp2/3 and phosphomyosin revealed a sharp boundary between the polar lobe neck (marked by phosphomyosin) and the polar lobe cortex (marked by Arp2/3) as early as phase I (Fig. 7A–D), and was particularly evident in early phase II and phase II embryos (Fig. 7E-L), when active myosin enrichment at the polar lobe neck was highest. This mutually exclusive localization of phosphomyosin and Arp2/3 suggested that Arp2/3 may

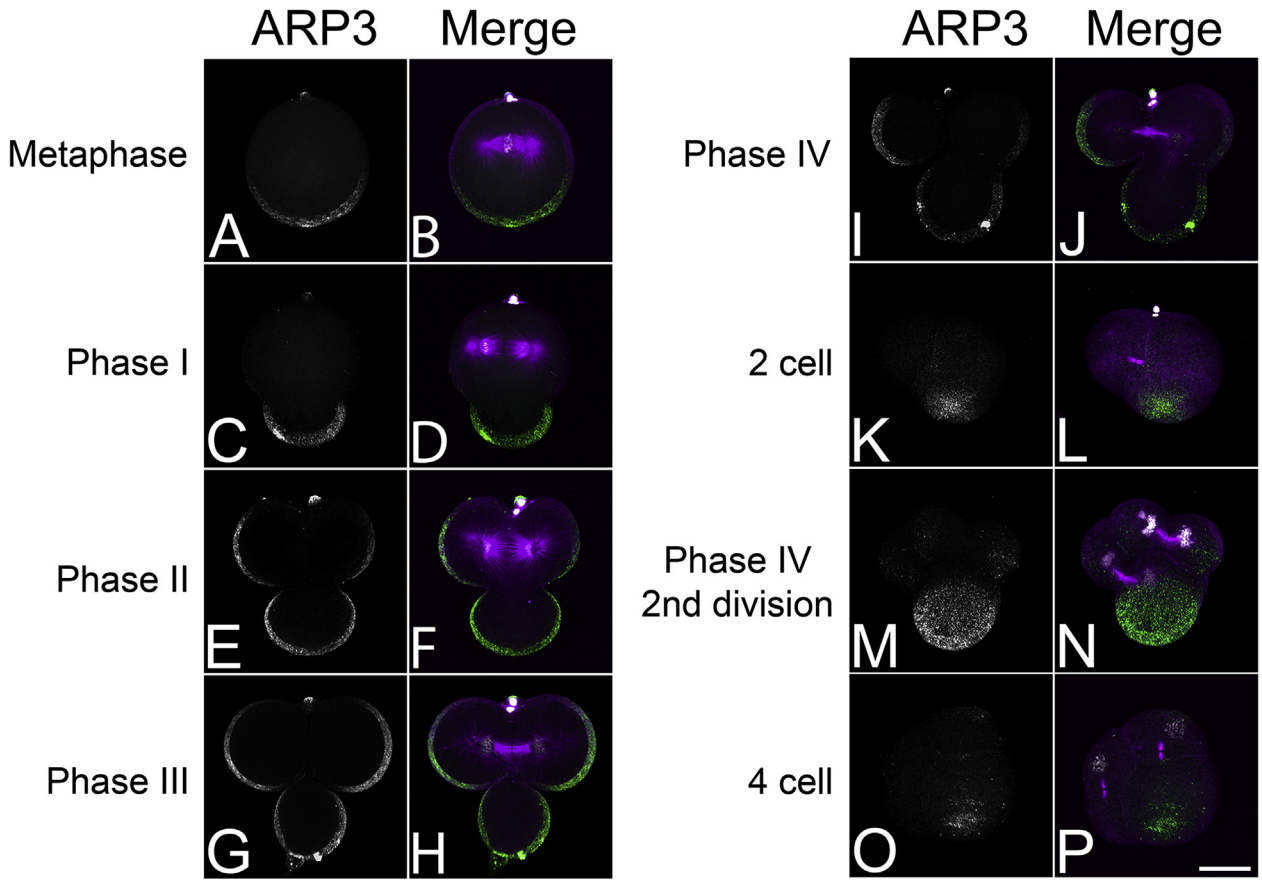

Fig. 6. Arp2/3 is enriched at the vegetal cortex during polar lobe formation. *C. hastata* embryos were processed for Arp2/3 (green), microtubules (magenta) and DNA (white) localization, and maximum projection images were generated by confocal microscopy. At first metaphase (A; panels a, b), when the zygote started to elongate, Arp2/3 was already marking the site of the future PL at the vegetal cortex. Arp2/3 was maintained at the vegetal pole during the first and second cell divisions, but excluded from both contractile ring and PL constriction zones (A; panels e–h, and B; panels c, d). This Arp2/3 zone was maintained through the second division (B), only to dissipate after the second division (B; panels e, f). Bars, 30 μm.

play a functional role in polar lobe formation, possibly by restricting cortical contractility in the lobe. To test this notion, embryos were treated following extrusion of the second polar body with CK666, an Arp2/3 inhibitor that we have previously demonstrated reversibly blocks dendritic actin nucleation and lamellipodia formation in other marine invertebrates (Henson et al., 2015; Sepúlveda-Ramírez et al., 2018). Carrier control (DMSO) or CK666-treated embryos were followed through the second cleavage by time-lapse microscopy (Fig. 8A). Inhibition of Arp 2/3 did not alter animal-vegetal elongation associated with Phase I, but polar lobe constriction never progressed past phase I (Fig. 8A, panels l–o). Instead, the cleavage plane appeared to shift such that the resulting AB blastomere was smaller than controls (Fig. 8A, panels g and p, Supplemental Movies 3 and 4). Although symmetrical or mitotic defects were also observed (Fig. 8B), the enlarged CD and smaller AB blastomeres was the major phenotype observed in embryos cultured in the presence of CK666 (Fig. 8B). Lastly, examination of microtubule morphology in control and CK666-treated embryos suggested that spindle morphology was not suggestive of a major qualitative disruption of central spindle organization, suggesting that this failure to achieve a proper polar lobe constriction was not a function of spindle disruption (Fig. S4).

Supplementary video related to this article can be found at https://doi.org/10.1016/j.ydbio.2019.08.020.

3. Discussion

The polar lobes formed by spiralian embryos have captured the imagination of embryologists and cell biologists for over a century. The transient sequestration of vegetal cortex through the first two embryonic divisions such that this domain is inherited by the CD macromere lineage is highly suggestive of a strong developmental role for the polar lobe. Yet ablation studies have resulted in very species-specific phenotypes (Cather and Verdonk, 1974; Crampton and Wilson, 1896; Henry, 1989; Henry et al., 2006; Wilson, 1904), and to date, there has yet to be a specific developmental determinant identified as being sequestered by the polar lobe. Thus, the precise developmental role for segregating vegetal cytoplasm remains somewhat mysterious. To the cell biologist, the polar lobe poses a different set of questions: 1) To what extent is the polar lobe constriction like a contractile ring?; and 2) if the cleavage plane is determined by factors associated with the mitotic apparatus, then how does the polar lobe constriction form in a plane perpendicular to the plane of cytokinesis? The data described in this report begins to shed some light on these open questions, using a combination of fixed and live cell analyses. We report that the CPC's core effector kinase Aurora B is required for polar lobe constriction past phase II, extending the earlier findings that microtubules are not required early in polar lobe formation (Conrad et al., 1992; Conrad and Conrad, 1992; Conrad and Williams, 1974; Raff, 1972). Additionally, for the first time we identify the Arp2/3 complex as a marker of the polar lobe cortex and establish that Arp2/3 is required for proper polar lobe formation. And while these findings generate a new set of questions regarding the spatiotemporal regulation of polar lobe formation, we now have an experimental foundation to further explore the parameters that control the execution of this highly atypical form of embryonic cell division.

Immunolabeling of actin and active myosin II at the contractile ring and PLC suggest that enrichment at the two planes of constriction occurs concomitantly during the first cell division in *Chlamys* embryos (Figs. 1

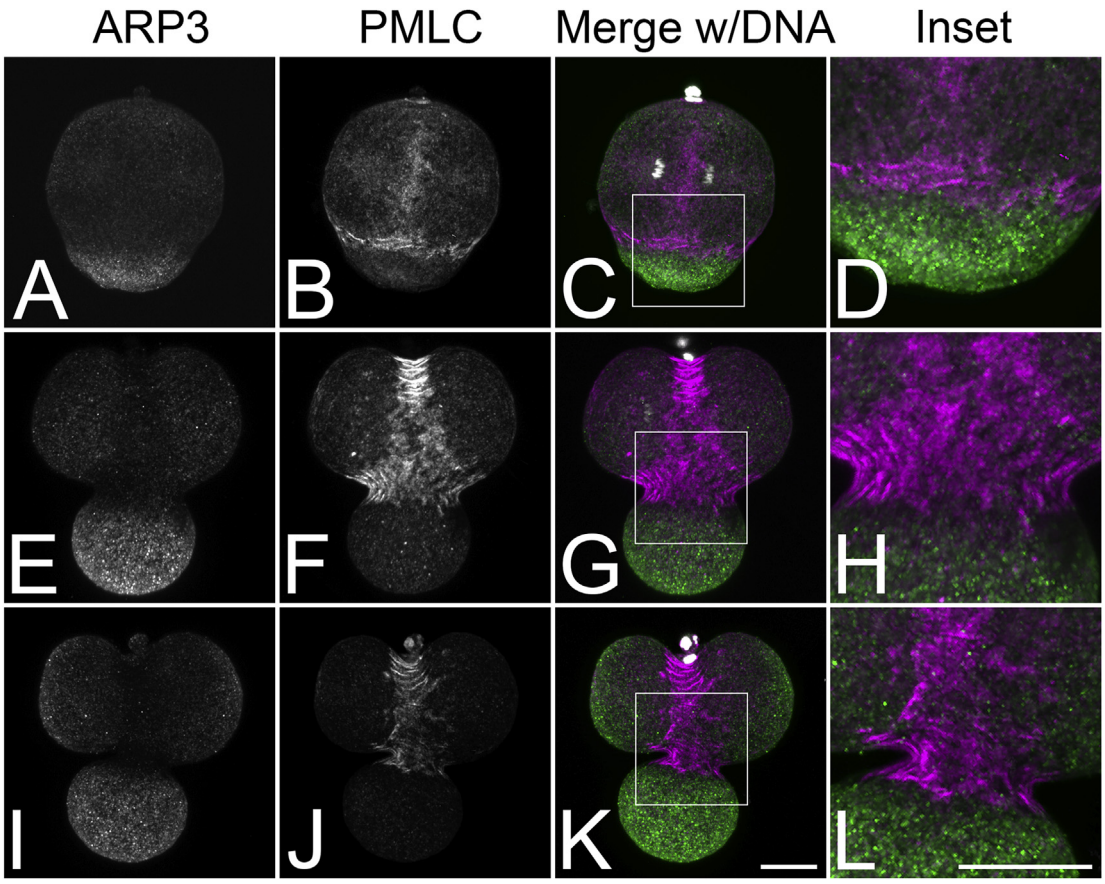

Fig. 7. Mutually exclusive localization of activated myosin II and Arp2/3 at the cleavage furrow and polar lobe neck. *C. hastata* embryos were processed for Arp2/3 (green), PMLC (magenta), and DNA (white) localization, and maximum projection images were generated by confocal microscopy. PMLC was present at the cleavage furrow and PLC, while Arp 2/3 was excluded from these contractile areas, confined to the polar regions of the two daughter cells and vegetal cortex of the polar lobe. Bar, 15 μm.

and 2). This is in agreement with previous descriptions of cortical actin being enriched at both the cleavage furrow and polar lobe constriction (Conrad and Williams, 1974; Conrad et al., 1973; Hejnol and Pfannenstiel, 1998; Raff, 1972; Schmidt et al., 1980). Disruption of actin filaments with cytochalasin B or Latrunculin B prevents the formation of both structures, although the PLC is more sensitive than the contractile ring to lower doses of these drugs (Conrad et al., 1992; Conrad and Williams, 1974; Raff, 1972). Similarly, it has been reported that the polar lobe is sensitive to myosin inhibition with 2,3-butanedione monoxime (BDM) (Hejnol and Pfannenstiel, 1998), although it should be noted that BDM also inhibits the Arp2/3 complex (Henson et al., 2009). Thus, in many respects, the polar lobe constriction structurally and functionally resembles a contractile ring. Yet despite these similarities between the contractile ring and PLC, there are several important differences between the two structures. The first is the differential requirement for microtubules. Like all animal cells, microtubules are required to break symmetry and establish the zone of active Rho that in turn directs the contractile ring assembly (Bement et al., 2005; Werner et al., 2007). Ablation of the spindle with microtubule poisons blocks furrow initiation in cells (Beams and Evans, 1940), presumably by preventing positioning of factors that define the cleavage plane such as the centralspindlin and CPC complexes (D'Avino et al., 2005; Glotzer, 2009). However, Phase I of polar lobe formation is independent of microtubules (Conrad et al., 1992; Conrad and Williams, 1974) in support of this notion, inhibition of the catalytic component of the chromosomal passenger complex (Aurora B kinase) had no effect on phase I but blocked further PLC ingression past phase II (Fig. 5). This suggests that the microtubules proximal to- or in contact with the phase III PLC may have central spindle-like properties that would further promote polar lobe neck constriction, thus taking on the features of a conventional contractile ring. Previous work in sea urchins suggest that microtubules decorated with centralspindlin and the CPC are differentially stable (Argiros et al., 2012), but those microtubules in direct contact with the PLC did not appear as stable as the central spindle, where the cytokinetic machinery is localized (Fig. 4). It is also possible that mere proximity of the central spindle to the lobe neck is enough to promote PLC ingression past phase II. Indeed, micromanipulation of sand dollar eggs such that one equatorial surface was conical in shape (thus mimicking a phase I constriction) induced a polar lobe-like constriction within the conical domain that was perpendicular to the cleavage plane (Rappaport and Rappaport, 1994). Localization of the CPC and centralspindlin complexes during polar lobe formation will establish whether the predictions suggested by Rappaport's conical cells represents a physiologically relevant model for how the polar lobe constriction is mechanistically linked to cytokinesis.

Another fundamental difference between contractile rings and PLC is that while the contractile ring ingresses to completion, the PLC relaxes to shunt the contents of the lobe into the CD blastomere. This may also be related to the lack of stable microtubule involvement with the PLC. During cytokinesis, there is a positive feedback loop between the components of the central spindle and the contractile ring that promotes stable ring constriction (Hu et al., 2008; Landino and Ohi, 2016), and at the end of the ring constriction, the bipolar central spindle assembles into a stable midbody. It may be that in the absence of a stable antiparallel microtubule array promoting a feedback loop and forming a midbody, the PLC cannot be maintained and regresses as the embryo re-enters interphase. Examination of the cytokinetic factors such as the CPC, centralspindlin and other midbody markers will hopefully lend insights into this question.

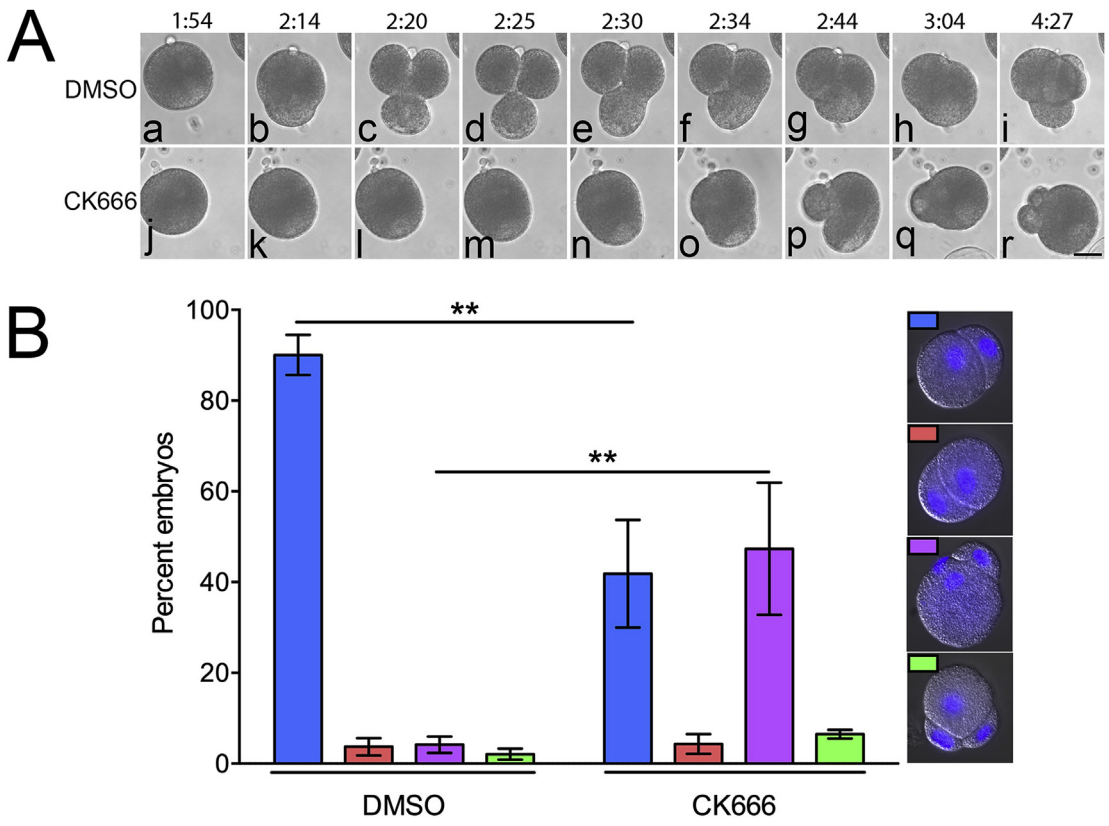

Fig. 8. Inhibition of Arp2/3 disrupts PL formation and daughter cell asymmetry. A) Time-lapse stills of *C. rubida* embryos that were treated with either 0.1% DMSO or 100 μM CK666 to inhibit Arp2/3 after completing second meiosis. While the initial vegetal elongation in the zygote was observed in treated embryos (k–m), further constriction of the polar lobe neck did not occur, resulting in a shift in the position of the spindle and cleavage plane (p) and an exaggerated asymmetric cell division compared to controls. Bar, 30 μm. **B)** Phenotypic analysis of embryos treated with either 0.1% DMSO or 100 μM CK666, and after first division fixed and stained with Hoechst 33342 to detect DNA. Wild-type (blue bar) embryos were characterized by a larger CD blastomere and a smaller AB blastomere. The frequency of embryos with symmetric blastomeres (red bar) was not affected by CK666 treatment, whereas there was a significant increase in embryos with highly asymmetrical blastomeres (magenta bar). A small but insignificant increase in 3 cell embryos (green bar) was also observed. Errors bar represent SD for three replicate experiments per condition, >50 embryos per experiment, $^{**}p < 0.01$ as determined by two-way ANOVA analysis.

Our demonstration that initiation of the polar lobe constriction is independent of microtubules and Aurora B kinase activity (Fig. 5) strongly suggests that there must be some additional spatial cues that help define the domain to be sequestered by the polar lobe. We have identified the actin-nucleating factor, Arp2/3, as one such candidate. Arp2/3 serves as an actin filament nucleator by binding to the sides of preexisting filaments and nucleating a second filament at a 70° angle to the parent filament (Rotty et al., 2013). These branched actin networks are critical for the formation of the lamellipodial region at the leading edge of motile cells (Pollard and Borisy, 2003), however the roles of Arp2/3 in isotropic actin networks such as the egg cortex are less clear. Our results demonstrate that in two scallop species and the oyster *Crassostrea gigas*, Arp 2/3 marked the vegetal pole of the egg cortex and site of future polar lobe, beginning as early as meiosis I (Figs. 6, 7, S2 and S3) persisting through until the end of the second division, after which vegetal Arp2/3 dissipated (Fig. 6O,P). In addition, pharmacological disruption of Arp2/3 function had profound effects on polar lobe formation and blastomere asymmetry (Fig. 8), lending support to the hypothesis that this cortical enrichment of Arp2/3, and presumably its associated branched actin network, is important in specifying the zone of cortex destined for sequestration in the polar lobe. It should be noted that during cytokinesis, Arp2/3 is cleared from the region of the contractile ring by the activity of the Centralspindlin component RacGAP1/Cyk-4 that inactivates Rac1 that in turn leads to the downregulation of Arp2/3 at the cell equator (Canman et al., 2008; Zhuravlev et al., 2017). Why branched actin needs to be cleared from a contractile zone is not yet clear, but a similar mechanism may be operating during polar lobe formation.

How might a zone of Arp2/3 delimit the cortex destined for the polar lobe? Examination of the distributions of Arp2/3 and active myosin II may provide a possible clue. As illustrated in Fig. 7, Arp2/3 and active myosin II are mutually exclusive in the region of the PLC and contractile ring, reflecting what is observed in crawling cells where Arp2/3 is localized to the lamellipodial branched networks at the leading edge whereas myosin II is found further back in the lamella and in the trailing tail, areas where actomyosin contraction is taking place (Blanchoin et al., 2014), and this mutually exclusive localization of Arp2/3 and myosin II is also observed at a more local level in growth cones (Yang et al., 2012). The notion that creating a zone enriched in Arp2/3-nucleated actin might place a spatial constraint on myosin II distribution is supported by *in vitro* studies, where myosin II displays a clear preference for anti-parallel networks over branched actin networks (Reymann et al., 2012). Thus, special enrichment of Arp2/3 (and thus branched actin networks) might create a less contractile or "softer" cortical domain, as has been observed in mouse oocytes where ectopic Arp2/3 activation clears myosin II from the cortex, lowering overall cortical tension (Chaigne et al., 2013). Creation of these "softer" domains at the cell poles and in the polar lobe might serve the dual function of constraining myosin II as well as conferring a cortex that is easier to deform. On a much smaller scale, the polar bodies extruded during meiosis may represent a similar scenario, given that Arp2/3 is similarly enriched in the polar bodies present in *Chlamys* and *Crassostrea* (Fig. 6, S2 and S3), as well as mouse oocytes (Leblanc et al., 2011). Thus, polar bodies and polar lobes may represent similar structures whereby Arp2/3 enrichment creates a zone of lowered

cortical tension that is coupled with myosin II-based constriction to effect a highly asymmetrical division.

Actin and microtubules have long been appreciated as participating in polar lobe formation, but this report is the first to identify a factor of any kind (structural or developmental) that is sequestered in the polar lobe or plays a role in its formation. Future work will focus on precisely characterizing and experimentally manipulating the actin cytoskeleton in the Arp2/3 zone of the forming polar lobe, as well as comparing and contrasting the structure and mechanics of the cytokinetic contractile ring versus the polar lobe constriction. These studies will contribute to our understanding of the mechanisms of normal, symmetric cell division and atypical, asymmetric cell division-like constrictions that form the polar lobe.

4. Materials and methods

4.1. Embryo culture

The scallops *Chlamys rubida*, *Chlamys hastata* and the oyster *Crassostrea gigas* were collected in the waters surrounding San Juan Island and used on site at the Friday Harbor Laboratories. Gametes were obtained by injecting 4 mM serotonin (Sigma, H7752) in Filtered natural Sea Water (FSW), into the gonads or the adductor muscle, and eggs were washed once with excess FSW and filtered through a 102 μm Nitex mesh before being fertilized with diluted sperm. Embryos were cultured in densities less than 0.4% (vol/vol) at 12–14 °C.

4.2. Pharmacological treatments

Embryos were exposed to 0.1% Dimethyl Sulfoxide (DMSO) or drug inhibitor after second meiosis and then incubated until the two or four cell stage. To inhibit branched actin polymerization by the Arp2/3 complex cells were incubated in the presence of 100 μM CK 666 (Tocris, 3950), based on previously reported conditions for using CK666 in sea star oocytes and sea urchin coelomocytes (Henson et al., 2015; Mori et al., 2014). To inhibit Aurora B kinase activity, embryos were incubated in a range of doses between 20 and 100 μM ZM447439 (Tocris, 2458), and 50 μM ZM 447439 was found to be the lowest dose that reduced Histone H3 phosphorylation and blocked cytokinesis (Fig. S1). To rapidly depolymerize microtubules 20 μM Nocodazole (Selleckchem, S2775) was added for 2 min prior to fixation (Foe and von Dassow, 2008).

4.3. Immunolocalization

Embryos were fixed and processed for immunolocalization as described (Argiros et al., 2012). Briefly, embryos were fixed in Millonig's Fixative (0.2 M NaH_2PO_4, 0.136 M NaCl, pH 7, 3.7% Formaldehyde) for 20 min at room temperature, followed by 3 washes of Phosphate-Buffered Saline with 0.1% Triton X-100 (PBST, 10 mM Na_2HPO_4, 137 mM NaCl, 2.7 mM KCl, 1.8 mM KH_2PO_4). Embryos were then rocked at room temperature for 1 h in blocking buffer solution (PBST + 5% BSA). Embryos were incubated in combinations of mouse monoclonal anti-Arp3 (1:200, Sigma, A5979), rabbit anti-phospho Ser19 myosin regulatory light chain (1:200, Cell Signaling, 3671S), rat anti-α tubulin (YL1/2) (1:1000, Santa Cruz Biotechnology, sc-53029) and rabbit anti-phosphohistone H3 Ser10 (1:300, Sigma, 9701S). Embryos were incubated in primary antibody overnight at 4 °C, washed 3 times with PBST and rocked overnight at 4 °C in Alexa Flour-labeled secondary antibodies (Life Technologies) along with 1 μg/ml Hoescht, to visualize DNA (Thermo Scientific, 62249). To visualize filamentous actin, Alexa Fluor 568 Phalloidin (Thermo Fisher Scientific, A12380) was included in the secondary antibody solution. Embryos were then washed and mounted in 90% glycerol in 1x PBS.

4.4. Image acquisition and analysis

For timelapse imaging of scallop embryos, embryos were cultured at 12 °C on a Brook cooling microscope stage mounted on a Nikon TS100 microscope, and phase contrast images were acquired every 60 s using a Spot Insight MP monochrome CCD camera. Fixed embryos were imaged by confocal microscopy using an Andor Dragonfly 550 spinning disc confocal microscope mounted on an Olympus IX83 inverted microscope, using a 60x N.A. 1.3 silicone objective. Z-stacks were acquired using a Zyla Plus 4.2 sCMOS camera driven by Fusion Software. For increased resolution of microtubules, single plane Super Resolution Radial Fluctuation (SRRF-Stream) images were acquired (Culley et al., 2018), with 100 frames acquired for each image. Bitplane Imaris (version 8.1–9.1.2) software was used to generate three-dimensional renderings from the acquired image stacks. Montages were prepared in Adobe Photoshop (CS).

For imaging of Phosphohistone H3 levels in control- and ZM447439-treated oocytes (Fig. S1), samples were imaged using a 40x Plan Apochromat, 1.3 NA objective mounted on an Axiovert 200M inverted microscope (Carl Zeiss, Thornwood, NY) equipped for epifluorescence microscopy and optical sectioning with an Apotome structured illumination module. Equivalent exposures were acquired for each channel, and montages were montages were prepared in Adobe Photoshop (CS) without any additional adjustments to the channel images.

4.5. Statistical analysis

Frequency data was transformed by applying arcsin-square root, followed by two-way Analysis of Variance (ANOVA) and a Tukey-Kramer post-hoc test utilizing Graphpad Prism 6 with a 95% confidence interval. Graphs were prepared in Graphpad Prism 6.

4.6. Key resources table

Reagent or resource	Source	Identifier
Antibodies		
Mouse monoclonal anti-Arp3	Sigma-Aldrich	Cat#A5979
Rabbit anti-phospho Ser19 myosin regulatory light chain	Cell signaling	Cat#3671S
Rat anti-αTubulin (YL1/2)	Santa Cruz Biotechnology	Cat#sc-53029
Rabbit anti-phosphohistone H3 Ser10	Sigma-Aldrich	Cat#9701S
Bacterial and Virus Strains		

(continued on next page)

(*continued*)

Reagent or resource	Source	Identifier
Biological Samples		
Chemicals, Peptides, and Recombinant Proteins		
Serotonin	Sigma-Aldrich	Cat#H7752
CK666	Tocris	Cat#3950
ZM447439	Tocris	Cat#2458
Nocodazole	Selleckchem	Cat#S2775
Critical Commercial Assays		
Deposited Data		
Experimental Models: Cell Lines		
Experimental Models: Organisms/Strains		
Chlamys rubida	San Juan Island, WA	N/A
Chlamys hastata	San Juan Island, WA	N/A
Crassostrea gigas	San Juan Island, WA	N/A
Oligonucleotides		
Recombinant DNA		
Software and Algorithms		
GraphPad Prism 6	Two-way ANOVA with Tukey-Kramer's post-hoc test; GraphPad Prism v6.00 for Apple, GraphPad Software, San Diego California USA.	www.graphpad.com
Other		

Acknowledgements

The authors want to thank Megan Dethier (FHL), Aaron Galloway (FHL), Ross Whippo (FHL), and Maria Rosa (Stonybrook University) for assistance in collecting animals. This work was supported by collaborative research grants from The National Science Foundation to J.H.H (MCB-1412688) and C.B.S. (MCB-1412734); and a National Institutes of Health grant R15HD080533 to C.B.S. L.T was supported by a Charles Lambert fellowship from the Friday Harbor Laboratories, and a grant from the National Council of Science and Technology in Mexico (CONACyT).

Appendix A. Supplementary data

Supplementary data to this article can be found online at https://doi.org/10.1016/j.ydbio.2019.08.020.

References

Argiros, H., Henson, L., Holguin, C., Foe, V., Shuster, C.B., 2012. Centralspindlin and chromosomal passenger complex behavior during normal and Rappaport furrow specification in echinoderm embryos. Cytoskeleton (Hoboken) 69, 840–853.

Atkinson, J.W., 1971. Organogenesis in normal and lobeless embryos of the marine prosobranch gastropod Ilyanassa obsoleta. J. Morphol. 133, 339–352.

Beams, H., Evans, T., 1940. Some effects of colchicine upon the first cleavage in Arbacia punctulata. Biol. Bull. 79, 188–198.

Bement, W.M., Benink, H.A., von Dassow, G., 2005. A microtubule-dependent zone of active RhoA during cleavage plane specification. J. Cell Biol. 170, 91–101.

Blanchoin, L., Boujemaa-Paterski, R., Sykes, C., Plastino, J., 2014. Actin dynamics, architecture, and mechanics in cell motility. Physiol. Rev. 94, 235–263.

Canman, J.C., Lewellyn, L., Laband, K., Smerdon, S.J., Desai, A., Bowerman, B., Oegema, K., 2008. Inhibition of Rac by the GAP activity of centralspindlin is essential for cytokinesis. Science 322, 1543–1546.

Carmena, M., 2008. Cytokinesis: the final stop for the chromosomal passengers. Biochem. Soc. Trans. 36, 367–370.

Carmena, M., Wheelock, M., Funabiki, H., Earnshaw, W.C., 2012. The chromosomal passenger complex (CPC): from easy rider to the godfather of mitosis. Nat. Rev. Mol. Cell Biol. 13, 789–803.

Cather, J.N., Verdonk, N.H., 1974. The development of Bithynia tentaculata (Prosobranchia, Gastropoda) after removal of the polar lobe. J. Embryol. Exp. Morphol. 31, 415–422.

Chaigne, A., Campillo, C., Gov, N.S., Voituriez, R., Azoury, J., Umaña-Diaz, C., Almonacid, M., Queguiner, I., Nassoy, P., Sykes, C., Verlhac, M.H., Terret, M.E., 2013. A soft cortex is essential for asymmetric spindle positioning in mouse oocytes. Nat. Cell Biol. 15, 958–966.

Clement, A.C., 1952. Experimental studies on germinal localization in Ilyanassa. I. The role of the polar lobe in determination of the cleavage pattern and its influence in later development. J. Exp. Zool. 121, 593–625.

Conrad, A.H., Paulsen, A.Q., Conrad, G.W., 1992. The role of microtubules in contractile ring function. J. Exp. Zool. 262, 154–165.

Conrad, A.H., Stephens, A.P., Conrad, G.W., 1994. Effect of hexylene glycol-altered microtubule distributions on cytokinesis and polar lobe formation in fertilized eggs of Ilyanassa obsoleta. J. Exp. Zool. 269, 188–204.

Conrad, G.W., Conrad, A.H., 1992. Microtubules as key cytoskeletal elements in cellular transport and shape changes: their expected responses to space environments. Trans. Kans. Acad. Sci. 95, 45–49.

Conrad, G.W., Williams, D.C., 1974. Polar lobe formation and cytokinesis in fertilized eggs of Ilyanassa obsoleta. I. Ultrastructure and effects of cytochalasin B and colchicine. Dev. Biol. 36, 363–378.

Conrad, G.W., Williams, D.C., Turner, F.R., Newrock, K.M., Raff, R.A., 1973. Microfilaments in the polar lobe constriction of fertilized eggs of Ilyanassa obsoleta. J. Cell Biol. 59, 228–233.

Crampton, H.E., Wilson, E.B., 1896. Experimental studies on gasteropod development. Arch. Entwicklungsmech. Org. 3, 1–19.

Culley, S., Tosheva, K.L., Matos Pereira, P., Henriques, R., 2018. SRRF: universal live-cell super-resolution microscopy. Int. J. Biochem. Cell Biol. 101, 74–79.

D'Avino, P.P., Savoian, M.S., Glover, D.M., 2005. Cleavage furrow formation and ingression during animal cytokinesis: a microtubule legacy. J. Cell Sci. 118, 1549–1558.

Ditchfield, C., Johnson, V.L., Tighe, A., Ellston, R., Haworth, C., Johnson, T., Mortlock, A., Keen, N., Taylor, S.S., 2003. Aurora B couples chromosome alignment with anaphase by targeting BubR1, Mad2, and Cenp-E to kinetochores. J. Cell Biol. 161, 267–280.

Foe, V.E., von Dassow, G., 2008. Stable and dynamic microtubules coordinately shape the myosin activation zone during cytokinetic furrow formation. J. Cell Biol. 183, 457–470.

Gadea, B.B., Ruderman, J.V., 2005. Aurora kinase inhibitor ZM447439 blocks chromosome-induced spindle assembly, the completion of chromosome condensation, and the establishment of the spindle integrity checkpoint in Xenopus egg extracts. Mol. Biol. Cell 16, 1305–1318.

George, O., Johnston, M.A., Shuster, C.B., 2006. Aurora B kinase maintains chromatin organization during the MI to MII transition in surf clam oocytes. Cell Cycle 5, 2648–2656.

Glotzer, M., 2005. The molecular requirements for cytokinesis. Science 307, 1735–1739.

Glotzer, M., 2009. The 3Ms of central spindle assembly: microtubules, motors and MAPs. Nat. Rev. Mol. Cell Biol. 10, 9–20.

Guerrier, P., Van den Biggelaar, J., Van Dongen, C., Verdonk, N., 1978. Significance of the polar lobe for the determination of dorsoventral polarity in Dentalium vulgare (da Costa). Dev. Biol. 63, 233–242.

Guse, A., Mishima, M., Glotzer, M., 2005. Phosphorylation of ZEN-4/MKLP1 by aurora B regulates completion of cytokinesis. Curr. Biol. 15, 778–786.

Gustafsson, N., Culley, S., Ashdown, G., Owen, D.M., Pereira, P.M., Henriques, R., 2016. Fast live-cell conventional fluorophore nanoscopy with ImageJ through super-resolution radial fluctuations. Nat. Commun. 7, 12471.

Hejnol, A., Pfannenstiel, H.D., 1998. Myosin and actin are necessary for polar lobe formation and resorption in Ilyanassa obsoleta embryos. Dev. Gene. Evol. 208, 229–233.

Henry, J.J., 1989. Removal of the polar lobe leads to the formation of functionally deficient photocytes in the annelidChaetopterus variopedatus. Roux's Arch. Dev. Biol. 198, 129–136.

Henry, J.Q., Lyons, D.C., Perry, K.J., Osborne, C.C., 2017. Establishment and activity of the D quadrant organizer in the marine gastropod Crepidula fornicata. Dev. Biol. 431, 282–296.

Henry, J.Q., Perry, K.J., Martindale, M.Q., 2006. Cell specification and the role of the polar lobe in the gastropod mollusc Crepidula fornicata. Dev. Biol. 297, 295–307.

Henson, J.H., Cheung, D., Fried, C.A., Shuster, C.B., McClellan, M.K., Voss, M.K., Sheridan, J.T., Oldenbourg, R., 2009. Structure and dynamics of an Arp2/3 complex-independent component of the lamellipodial actin network. Cell Motil. Cytoskelet. 66, 679–692.

Henson, J.H., Yeterian, M., Weeks, R.M., Medrano, A.E., Brown, B.L., Geist, H.L., Pais, M.D., Oldenbourg, R., Shuster, C.B., 2015. Arp2/3 complex inhibition radically alters lamellipodial actin architecture, suspended cell shape, and the cell spreading process. Mol. Biol. Cell 26, 887–900.

Hu, C.K., Coughlin, M., Field, C.M., Mitchison, T.J., 2008. Cell polarization during monopolar cytokinesis. J. Cell Biol. 181, 195–202.

Landino, J., Ohi, R., 2016. The timing of midzone stabilization during cytokinesis depends on myosin II activity and an interaction between INCENP and actin. Curr. Biol. 26, 698–706.

Leblanc, J., Zhang, X., McKee, D., Wang, Z.B., Li, R., Ma, C., Sun, Q.Y., Liu, X.J., 2011. The small GTPase Cdc42 promotes membrane protrusion during polar body emission via ARP2-nucleated actin polymerization. Mol. Hum. Reprod. 17, 305–316.

Lu, M.S., Johnston, C.A., 2013. Molecular pathways regulating mitotic spindle orientation in animal cells. Development 140, 1843–1856.

Morgan, T.H., 1933. The formation of the antipolar lobe in Ilyanassa. J. Exp. Zool. 64, 433–467.

Mori, M., Somogyi, K., Kondo, H., Monnier, N., Falk, H.J., Machado, P., Bathe, M., Nédélec, F., Lénárt, P., 2014. An Arp2/3 nucleated F-actin shell fragments nuclear membranes at nuclear envelope breakdown in starfish oocytes. Curr. Biol. 24, 1421–1428.

Morin, X., Bellaïche, Y., 2011. Mitotic spindle orientation in asymmetric and symmetric cell divisions during animal development. Dev. Cell 21, 102–119.

Novikoff, A.B., 1940. Morphogenetic substances or organizers in annelid development. J. Exp. Zool. 85, 127–155.

Pollard, T.D., Borisy, G.G., 2003. Cellular motility driven by assembly and disassembly of actin filaments. Cell 112, 453–465.

Raff, R.A., 1972. Polar lobe formation by embryos of Ilyanassa obsoleta. Effects of inhibitors of microtubule and microfilament function. Exp. Cell Res. 71, 455–459.

Rappaport, R., 1996. Cytokinesis in Animal Cells. Cambridge University Press.

Rappaport, R., Rappaport, B.N., 1994. Cleavage in conical sand dollar eggs. Dev. Biol. 164, 258–266.

Render, J., 1989. Development of Iiyanassa obsoleta embryos after equal distribution of polar lobe material at first cleavage. Dev. Biol. 132, 241–250.

Reymann, A.C., Boujemaa-Paterski, R., Martiel, J.L., Guérin, C., Cao, W., Chin, H.F., De La Cruz, E.M., Théry, M., Blanchoin, L., 2012. Actin network architecture can determine myosin motor activity. Science 336, 1310–1314.

Rotty, J.D., Wu, C., Bear, J.E., 2013. New insights into the regulation and cellular functions of the ARP2/3 complex. Nat. Rev. Mol. Cell Biol. 14, 7.

Schmidt, B.A., Kelly, P.T., May, M.C., Davis, S.E., Conrad, G.W., 1980. Characterization of actin from fertilized eggs of Ilyanassa obsoleta during polar lobe formation and cytokinesis. Dev. Biol. 76, 126–140.

Sepúlveda-Ramírez, S.P., Toledo-Jacobo, L., Henson, J.H., Shuster, C.B., 2018. Cdc42 controls primary mesenchyme cell morphogenesis in the sea urchin embryo. Dev. Biol. 437, 140–151.

Tyler, A., 1930. Experimental production of double embryos in annelids and mollusks. J. Exp. Zool. 57, 347–407.

Werner, M., Munro, E., Glotzer, M., 2007. Astral signals spatially bias cortical myosin recruitment to break symmetry and promote cytokinesis. Curr. Biol. 17, 1286–1297.

White, E.A., Glotzer, M., 2012. Centralspindlin: at the heart of cytokinesis. Cytoskeleton (Hoboken) 69, 882–892.

Wilson, E.B., 1904. Experimental studies on germinal localization. I. The germ-regions in the egg of Dentalium. J. Exp. Zool. 1, 1–72.

Yang, Q., Zhang, X.F., Pollard, T.D., Forscher, P., 2012. Arp2/3 complex-dependent actin networks constrain myosin II function in driving retrograde actin flow. J. Cell Biol. 197, 939–956.

Zhuravlev, Y., Hirsch, S.M., Jordan, S.N., Dumont, J., Shirasu-Hiza, M., Canman, J.C., 2017. CYK-4 regulates Rac, but not Rho, during cytokinesis. Mol. Biol. Cell 28, 1258–1270.